Medical Infrared Imaging (Thermography) of Type I Thoracolumbar Disk Disease in Chondrodystrophic Dogs

Brian P. Grossbard[1], DVM, Catherine A. Loughin[1,2], DVM, Diplomate ACVS and ACCT, Dominic J. Marino[1,2], DVM, Diplomate ACVS and ACCT, CCRP, Leonard J. Marino[1,2], MD, FAAP, Joseph Sackman[2], Scott E. Umbaugh[2,3], BSE, MSEE, PhD, Patrick S. Solt[2,3], BSEE, MSCS, Jakia Afruz[3], BSAPECE, MSAPECE, Peter Leando[2,4], PhD, DSc, DAc, Martin L. Lesser[2,5], PhD, EMT-CC, and Meredith Akerman[5], MS

[1] Department of Surgery, Long Island Veterinary Specialists, Plainview, New York ,[2] The Canine Chiari Institute at Long Island Veterinary Specialists, Plainview, New York ,[3] Computer Vision and Image Processing Laboratory, Electrical and Computer Engineering Department, Southern Illinois University at Edwardsville, Edwardsville, Illinois ,[4] Meditherm, Inc., Fort Myers, Florida and [5] North Shore—LIJ Health System Feinstein Institute for Medical Research, Biostatistics Unit, Manhasset, New York

Corresponding Author
Dominic J. Marino, DVM, Diplomate ACVS, ACCT and CCRP, The Canine Chiari Institute at Long Island Veterinary Specialists, 163 South Service Road, Plainview, NY 11803.
E-mail: bongorno@aol.com

Submitted January 2011
Accepted August 2011

DOI:10.1111/j.1532-950X.2014.12239.x

Objective: To: (1) determine the success of medical infrared imaging (MII) in identifying dogs with TLIVDD, (2) compare MII localization with magnetic resonance imaging (MRI) results and surgical findings, and (3) determine if the MII pattern returns to that of normal dogs 10 weeks after decompression surgery.
Study Design: Prospective case series.
Animals: Chondrodystrophic dogs (n = 58) with Type I TLIVDD and 14 chondrodystrophic dogs with no evidence of TLIVDD.
Methods: Complete neurologic examination, MII, and MRI studies were performed on all dogs. Dogs with type I TLIVDD had decompressive surgery and follow-up MII was performed at 10 weeks. Pattern analysis software was used to differentiate between clinical and control dogs, and statistical analysis using anatomic regions of interest on the dorsal views were used to determine lesion location. Recheck MII results were compared with control and pre-surgical images.
Results: Computer recognition pattern analysis was 90% successful in differentiating normal dogs from dogs affected by TLIVDD and 97% successful in identifying the abnormal intervertebral disc space in dogs with TLIVDD. Statistical comparisons of the ROI mean temperature were unable to determine the location of the disc herniation. Recheck MII patterns did not normalize and more closely resembled the clinical group.
Conclusions: MII was 90% successful differentiating between normal dogs and 97% successful in identifying the abnormal intervertebral disc space in dogs with TLIVDD. Abnormal intervertebral disc space localization using ROI mean temperature analysis was not successful. MII patterns 10 weeks after surgery do not normalize.

Acute thoracolumbar intervertebral disk rupture secondary to Hansen Type I intervertebral disk disease is a common cause of neurologic dysfunction in dogs. Clinical signs result from extrusion of disk material into the vertebral canal and compression of the spinal cord and or nerve roots. Types of clinical signs vary from spinal hyperesthesia, ataxia, paraparesis, or paralysis, with or without deep pain perception, and urinary and fecal incontinence.[1–6] Neurologic deficits in dogs with thoracolumbar intervertebral disk rupture are generally limited to the pelvic limbs; however, occasional thoracic limb abnormalities can be noted with Schiff-Sherrington syndrome.[1–6,7] Intervertebral disk degeneration and subsequent herniation is especially prevalent in chondrodystrophoid breeds (e.g., Dachshund, Poodle, Pekingese, Beagle, Welsh Corgi, Cocker Spaniel), and usually occurs between 2 and 8 years of age.[2–4,6–9]

Diagnosis of thoracolumbar intervertebral disk disease (TLIVDD) is based on history, signalment, clinical signs, and diagnostic imaging findings. Differential diagnosis includes trauma, acute spinal ischemia (fibrocartilaginous embolism), diskospondylitis, vertebral malformation, or neoplasia.[2,4,7,8] Whereas neuroanatomic localization can be determined from neurologic examination, identifying the specific cause necessitates advanced diagnostic imaging and sometimes biopsy.[2–4,7]

Diagnostic imaging modalities used in dogs with TLIVDD include: contrast myelography, computed tomography (CT), and magnetic resonance imaging (MRI). MRI is considered the method of choice for imaging the nervous system in people and is becoming the preferred diagnostic modality in veterinary medicine. Advantages of MRI include excellent soft tissue definition and the ability to provide prognostic information.[4,6,8,10–12] Disadvantages of MRI

include cost, requirement for general anesthesia, and limited availability and these factors limit routine use of MRI as a diagnostic imaging modality in veterinary medicine.[11–13]

Medical infrared imaging (MII) or thermography is a non-invasive imaging modality used to detect abnormal physiologic changes in people and animals.[14–49] Medical infrared imaging cameras record the emission of surface heat from the skin and generate thermal patterns in the form of a color map. Regions of elevated temperature are related to an increase in local circulation and metabolic rate, and can be clinically associated with inflammation, whereas regions of decreased temperature can clinically be associated with decreased tissue perfusion secondary to a vascular shunt, infarction, or changes in the autonomic nervous system.[14–16] Local dermal microcirculation, directly controlled by the sympathetic portion of the autonomic nervous system, is responsible for the surface heat detected,[14,17] not heat emanating from deeper tissues. Any condition that results in changes in sympathetic tone can alter cutaneous perfusion, thus changing the thermographic color map. Therefore, MII is a screening test, not a specific test. This explains the successful use of MII in patients of all sizes regardless of the presence of excessive body fat.[17]

MII systems have become increasingly sophisticated incorporating focal plane array detectors with high-speed images and spatial resolution.[17] Image recognition software is being developed for objective analysis of thermal patterns.[18] MII has been evaluated as a diagnostic modality for a wide range of conditions in human medicine, most commonly orthopedic[18–22] or neurologic[23–27] injuries, neoplasia,[18,28] and vascular disorders.[29] The normal thermogram of a human spine has been characterized by a central zone of decreased heat emanation in the region of the spinal processes from the cervical spine down to the lower lumbosacral spine.[23] The clinical level of intervertebral disk herniation can be localized in people with multiple sites of intervertebral disk disease and MII may play a role in selecting patients for advanced imaging.[26] Pathologic alterations in the thermal image patterns have included focal changes in temperature (increased initially, then decreased with chronicity) over the site of an active lesion and asymmetrical hyperthermia or hypothermia distal to the lesion.[23,26] Advantages of MII include non-invasiveness, relatively low cost, lack of exposure to ionizing radiation, lack of anesthetic requirement, and absence of adverse effects.

In veterinary medicine, MII has been used to evaluate a variety of disease conditions affecting llamas and cattle for infectious[30–33] and reproductive[34–36] diseases. Its application in equine medicine has been more diverse including: disorders of the tendons and ligaments, hoof (laminitis and navicular bone disease), joints, long bones and pelvic limb muscles, and the spine.[16,18,37–39,42,45]

Normal thermographic patterns of the canine limbs have been reported.[37] MII with computerized image recognition pattern analysis has been successful in differentiating between normal and cranial cruciate ligament deficient stifles in dogs.[41] In addition, pattern alterations in thermographic images have been documented in an experimental spinal cord injury model in dogs. In that study, the experimental sites were initially hyperthermic; however, they progressed to hypothermia within 1 week of injury. Significant changes between thoracic and lumbar temperatures were noted for 3 weeks after experimental spinal cord injury.[49] Similar imaging patterns would be expected in dogs clinically affected by acute TLIVDD.

We are unaware of published reports evaluating the use of MII for the diagnosis and localization of spontaneous intervertebral disk disease in dogs. Our purposes were to: (1) determine the success of MII in identifying dogs with TLIVDD; (2) compare the MII localization with MRI results and surgical findings; and (3) determine if the MII pattern returns to that of normal dogs 10 weeks after decompression surgery. We hypothesized that MII with computerized image recognition pattern analysis would be a useful screening tool for IVDD, thermographic lesion localization would correspond with MRI results and surgical findings, and that the thermographic pattern would return to normal 10 weeks after surgery.

MATERIALS AND METHODS

Case Selection Criteria

Between May 2009 and July 2010, consecutive small breed (<22 kg) chondrodystrophic dogs (n = 72), presenting with acute onset T3–L3 myelopathy and confirmed presence of TLIVDD on MRI were included in this study. Dogs that had been previously been treated for signs attributable to spinal cord disease or had previously undergone spinal surgery were excluded. Dogs were also excluded if diagnostic imaging revealed evidence of co-morbid disease that may have affected image interpretation (i.e., hemivertebrae, syringomyelia, embolism, neoplasia) or if no abnormalities were noted.

Control Dogs

Fourteen small breed chondrodystrophic dogs with no history of back or neck pain were evaluated in a similar manner to obtain a baseline normal MII for comparison. Each dog had a complete neurologic examination, MII, and a thoracolumbar MRI examination using the same protocol for the clinical patients.

Examination and Procedures

An initial physical and neurologic examination was performed on each dog before enrollment in the study. Neurologic examinations were performed by a Diplomate of the American College of Veterinary Internal Medicine (Neurology) or the American College of Veterinary Surgeons. Each dog's neurologic status was assigned a score based on a modification of the scale published by Wheeler and Sharp[50] (Table 1). Age, sex, body weight, body condition score, duration of clinical signs, and any previous medical therapy administered were recorded for each dog upon admission.

Dogs were allowed to acclimate to the room temperature of 70°F (21°C) for 30 minutes before MII. After this period,

Table 1 Neurologic Scale Modified From Wheeler and[Q1] Sharp[50]

Grade 0	Normal
Grade 1	Thoracolumbar pain, hyperesthesia
Grade 2	Paresis with decreased proprioception, ambulatory
Grade 3	Severe paresis with absent proprioception, not ambulatory
Grade 4	Paralysis, decreased, or no bladder control, deep pain perception present
Grade 5	Paralysis, urinary, and fecal incontinence, no deep conscious pain perception

small ink marks were placed on the dog's hair to the far left and right of specified locations between the T13–L1 and L7–S1 intervertebral disk spaces, outside the MII region of interest (ROI). Frozen metallic EKG clips were attached to the hair at these spots immediately before performing MII to provide thermographically recognizable anatomic landmarks. Locations were verified radiographically and correlated with the corresponding intervertebral disk spaces. In a pilot study (unpublished data), we showed that the presence of the clips did not significantly alter the MII pattern. To minimize thermal artifacts, manual contact was limited, and trained technicians wearing latex gloves handled all dogs by the head, neck, and ventral abdomen. A thermo-neutral fabric was used to support the caudal portion of the dogs if they were unable to stand on their own.

Images were obtained using an infrared camera (Med 2000 IRIS, Meditherm, Inc., Beaufort, NC) with a focal plane array amorphous silicone microbolometer. For real time data analysis the camera was connected to a laptop computer. To minimize background artifact, potentially created by temperature differences in exterior walls, the dogs were positioned in front of a uniform interior wall for all views in a custom designed MII suite. MII of the dorsal view (D1) and right (RL) and left (LL) lateral views (Fig 1A–C) were obtained. The dorsal view ROI extended from the caudal cervical region to the base of the tail. The ROI of the lateral views included the caudal cervical region and entire lateral body surface. The distance from the camera to the dogs was ~1 m for the dorsal images and 1.5 m for the lateral views. The markers were removed after image acquisition.

Meditherm software (Meditherm, Inc.) was used to save, analyze, review image data and calculate the mean, maximum and minimum temperatures of each ROI. Images were converted from black and white to a preset 8°C temperature scale and a 16-shade color map. We chose white and red to represent warmer temperatures and blue and black for cooler temperatures. Custom image recognition software (CVIPtools, Computer Vision and Image Processing Laboratory, Department of Electrical and Computer Engineering, School of Engineering, Southern Illinois University, Edwardsville, IL) was used to perform computer recognition pattern analysis (CRPA) and to compare thermographic patterns of dogs with TLIVDD to those of normal dogs.

Dogs were premedicated with subcutaneous hydromorphone (0.1 mg/kg) and atropine (0.4 mg/kg). General anesthesia was induced with telazol (2.2 mg/kg intravenously [IV]) and maintained with isoflurane in oxygen. After induction,

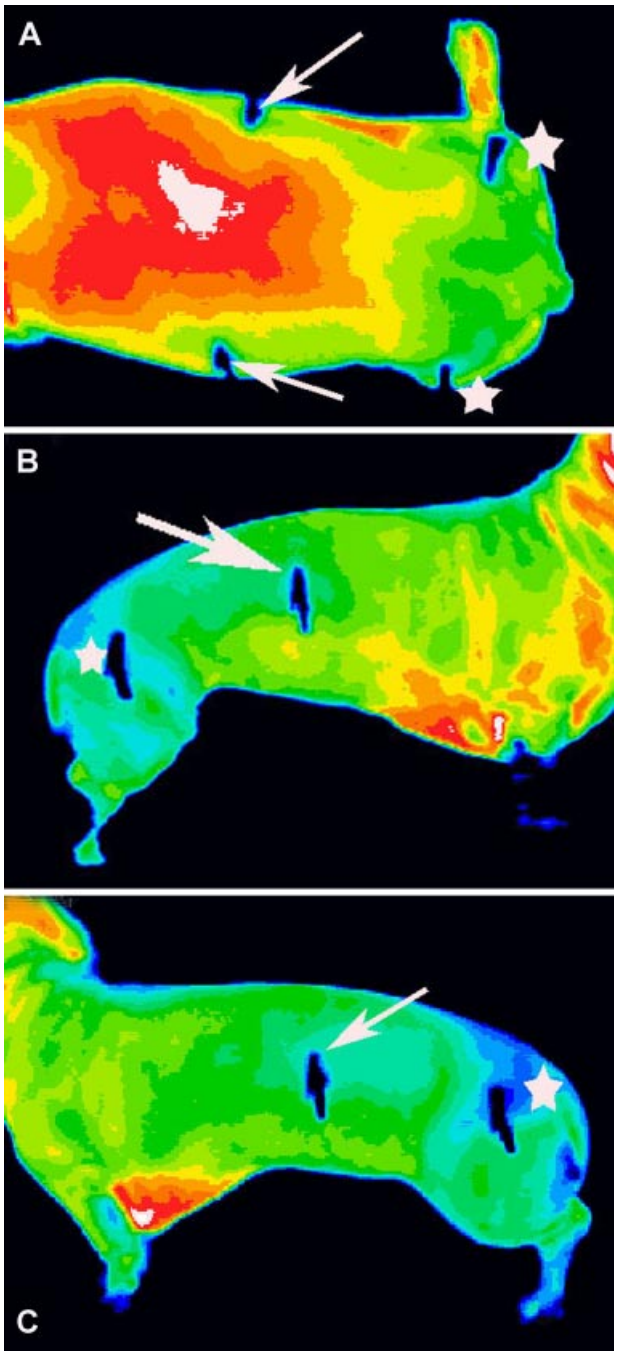

Figure 1 Medical infrared imaging of the dorsal view (A; D1), right (B; RL) and left (C; LL) lateral views of a 10-year-old female spayed Dachshund with grade III neurologic deficits secondary to a herniated intervertebral disc at L4–5 on the left. Note the hypothermic (blue) marking clips at the thoracolumbar junction (arrows) and lumbosacral space (stars).

dorsoventral and lateral radiographs were obtained with the metallic clips attached at the previously marked spots to document the locations of the thermographic markers. The markers were removed after radiographic imaging. Sagittal and

transverse MR images of the thoracolumbar spinal cord extending from C7 to S3 were obtained (Philips 3.0 Tesla magnet, Philips Healthcare, Andover, MA). The imaging protocol consisted of fast-spin echo (FSE) T2-weighted (T2-w) images in the sagittal (TE-76 ms, TR-4000 ms, slice thickness1.3 mm, gap 0.3 mm) and transverse (TE-120 ms, TR-3500 ms, slice thickness-2 mm, gap 0.5 mm) planes. The images were analyzed for evidence of intervertebral disk disease or other spinal pathology. MR images were interpreted by 2 authors (D.M. and C.L.) and a determination was made regarding the site of intervertebral disk herniation. All study dogs had decompressive hemilaminectomy and the results of MRI and surgical findings were recorded.

Dogs were assessed 2 weeks after discharge by neurologic evaluation and 10 weeks after discharge by neurologic evaluation and MII using the protocol previously described. Information recorded included neurologic grade (0–5), duration of physical therapy performed postoperatively, and current treatments.

Image Pattern Analysis

The Computer Vision and Image Processing Tools (CVIP tools) software was used to evaluate and analyze the images. The primary tools used include Analysis Features and Analysis Pattern Classification. The features considered include histogram and texture features. The histogram features include mean ± SD, skew, energy, and entropy; and the texture features include energy, inertia, correlation, inverse difference, and entropy. The pattern classification tools used include various normalization methods, distance and similarity measure and 3 classification methods. Additionally, software was modified to preprocess the images with 5 color normalization methods: (1) no normalization, (2) luminance, (3) normalized gray, (4) normalized RGB, and (5) normalized RGB luminance.

Dorsal MII images were divided into ROI based on the markings recorded during image acquisition and location of the TLIVDD. The ROI were the T9–10, T11–12, T13–L1, L2–3, L4–5, and L6–7 (Fig 2).

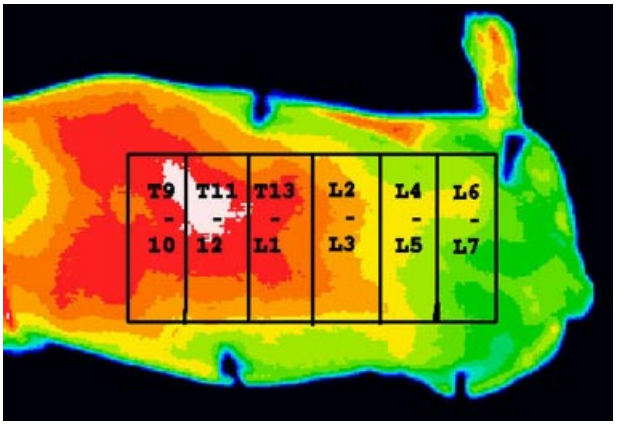

Figure 2 Medical infrared image of the dorsal view of the dog in Fig 1 divided into regions of interest. The regions of interest were the T9–10, T11–12, T13–L1, L2–3, L4–5, L6–7 vertebrae.

Experiments were run to classify each segment as affected or not affected with IVDD. These lesion localizations were compared to the MRI and surgical findings. The enhanced mask creation software was used for the project. This enhanced software facilitates the creation of a large number of masks. Additionally, algorithms were developed with the CVIP-ATAT for automatic mask creation. The new tool for feature extraction and pattern classification, CVIP-FEPC, was used extensively. It has been enhanced to perform leave-one-out experimental testing, and to automatically perform many combinations and permutations of an experiment with a single run. The new texture feature extraction software includes the 5 features that have been found to be the most useful: energy (homogeneity), inertia (contrast), correlation (linearity), inverse difference (local homogeneity), and entropy. The ATAT software allows the user to select from a set of image processing filters, segmentation methods, morphologic filters, and various post-processing imaging functions. The user is able to specify the range and the increment to be used with each of the imaging functions' parameters. The software will then automatically run all the possible algorithmic permutations. The success measure will be tailored to the specific application. Here, the CVIP-ATAT was used to develop algorithms to automatically create mask for the regions of interest. The color normalization software allows for the conversion of the original thermographic images into 4 color normalized mathematical spaces: (a) luminance, (b) normalized gray, (c) normalized RGB, (d) normalized RGB luminance. This conversion is based on the temperature data provided by the Meditherm software.

ROI Mean Temperature Analysis

Descriptive statistics (mean ± SD) were calculated for each anatomic section of the dogs or ROI. MII measurements of the mean temperature in the ROI "clinical" dogs were compared with control dogs using the 2 sample *t*-test. To measure variation within a dog, the coefficient of variation (CV) was calculated for the ROI of the thoracic and lumbar region of the spine. The rationale for using the CV was that if there was uniformity of temperature across the subregions of a dog, then the CV would be small relative to the CV of a dog having large variation in temperature across subregions. A result was considered statistically significant if $P < .05$. No adjustments for multiple testing were made. 95% confidence intervals for the differences in means between control and clinical were computed using standard asymptotic methods.

RESULTS

Clinical Findings

Fifty-eight dogs (33 male, 25 female) met the inclusion criteria. Dogs ranged from 1 to 13 years (mean, 5.6 years). There were 34 Dachshunds, 5 Beagles, 6 mix-breed dogs, 2 Bichon Frises, 2 Lhasa Apsos, 2 Maltese, 2 Pekingese and 2 Shih-Tzu, 1

Chihuahua, 1 Cocker Spaniel and 1 Havenese. Mean weight was 7.87 kg (range, 2.72–21.36 kg). On admission, 1 dog was classified as having grade 1 deficits, 21 dogs as grade 2 deficits, 17 as grade 3 deficits, 17 as grade 4 deficits, and 2 as grade 5 deficits. Mean neurologic grade was 2.96.

Fourteen dogs (7 male, 7 female; mean age, 3.2 years [range, 1–5.5 years], mean weight, 5.74 kg [range, 2.5–14.54 kg]) were included. There were 5 mix-breed dogs, 3 Chihuahuas, and 1 Bichon Frise, 1 Dachshund, 1 Italian Greyhound, 1 Miniature Pinscher, 1 Pomeranian, and 1 Yorkie.

A total of 58 MRI studies were evaluated in the clinical group. Sites of intervertebral disk herniation were T10–11 (n = 1), T11–12 (n = 8), T12–13 (n = 15), T13–L1 (n = 12), L1–2 (n = 8), L2–3 (n = 5), L3–4 (n = 4), and L4–5 (n = 5). There was 100% agreement between the location of the intervertebral disk herniation based on MRI and surgical findings.

Twenty-one dogs with TLIVDD dogs returned for recheck MII 10 weeks after surgery. Mean time between initial and recheck thermographic images was 66 days (range, 60–72 days). At the time of recheck examination, 6 dogs were classified as having grade 0 deficits, 9 dogs with grade 1 deficits, 4 dogs with grade 2 deficits, 1 dog with grade 3 deficits, 0 dogs with grade 4 deficits, and 1 dog was classified as having grade 5 deficits. Mean neurologic grade was 1.19.

There was a statistically significant difference between the ROI mean temperature in control dogs versus clinical dogs for CV thoracic (1.80 vs. 1.08, respectively, $P < .0265$), D1 L1LR min (24.95 vs. 23.04, respectively, $P < .0229$), D1 L1R min (26.58 vs. 24.36, respectively, $P < .0130$), D1 L full min (24.15 vs. 22.44, respectively, $P < .0410$), D1 R full min (24.67 vs. 22.82, respectively, $P < .0303$), and T11–12 R max (28.96 vs. 31.26, respectively, $P < .0490$; see Supplemental Table S1, online).

Computer recognition pattern analysis was ~90% successful identifying dogs with TLIVDD versus control dogs. The best classification results were 88.5% for the dorsal views, 89.8% for the left lateral view and 89.7% for the right lateral view. When the dorsal images were divided in to ROI, 97% of the vertebral segments were correctly classified as affected versus non-affected by IVDD (Table 2).

The image pattern comparison between the clinical group, the recheck clinical group and the control group was not statistically different between the clinical and control group classes. However, the recheck class results were more similar to the clinical group than the control group.

DISCUSSION

ROI Mean Temperature

There was a statistically significant difference between the ROI mean temperature in control dogs versus dogs with TLIVDD; however, it should be noted that because of the large number of statistical tests performed and the fact that the *P* values for the significant results ranged from ~ $P < .01$ to .04, some or all of these significant results may be spurious. It is common to make an adjustment to what is considered statistically significant in situations like this. If, for example, a so-called Bonferroni adjustment were made, none of these results would have been declared statistically significant. Although the average temperature was measured in smaller sub-regions based on neuroanatomic localizations in an effort to enhance accuracy of the temperature measurements for each region, a dilutional effect still occurs when dealing with focal areas of temperature difference that may be 50 pixels within a larger area or ROI that may be thousands of pixels. When averaging temperatures over the ROI, differences were not found to be significant between control dogs and dogs with TLIVDD. Creating smaller clinically relevant ROI may yield different results, but analysis may prove too time consuming and impractical in a clinical setting. Because of the aforementioned analysis limitations with averaging temperatures in ROI, localization of the specific intervertebral disk herniation was not successful in dogs with TLIVDD with this method.

Computer Recognition Pattern Analysis

Computer recognition pattern analysis was successful in differentiating normal dogs from dogs affected by TLIVDD. Dorsal and lateral images were equally useful for differentiating the clinical and normal dogs based on the classification being ~90%. Based on our results, MII could be used to "screen test" dogs suspected of having TLIVDD. Not only does MII not require general anesthesia, but it is substantially less

Table 2 Summary of the Computer Recognition Pattern Analysis Ability to Correctly Classify the Affected Intervertebral Space in Dogs With TLIVDD

Best Classification Results Features (Texture Pixel Dist = 5)	Data Normalization Method	Classification Method	Test Method	Number Correct in Test Set	Percent Correct
Histogram energy texture energy texture inertia texture inv-diff Texture entropy	Softmax r = 1	MLP (Partek, CVIP-FEPC selected features)	Leave K out, K = 10	220/226	97.3%
Histogram energy Texture energy Texture inertia Texture inv-diff Texture entropy	Softmax r = 1	Bayesian linear diskriminant (Partek, CVIP-FEPC selected features)	Train/test set	115/124	92.7%
Spectral 3 × 3 texture energy texture correlation texture entropy histogram SD histogram skew histogram energy histogram entropy	Standard normal density	K-Nearest neighbor K = 8 (CVIP-FEPC)	Leave-one-out	187/247	75.7%

expensive than CT with myelogram or MRI and may help clinicians identify the ROI in dogs undergoing advanced imaging and possibly surgery. MII has also been successful in identifying temperature changes associated with a pathology before the appearance of clinical symptoms by detecting alterations in perfusion.[30] Screening dogs with a history typical of dogs with TLIVDD may afford clinicians additional information relevant to developing a diagnostic and therapeutic plan. The thermographic patterns we found in control dogs were noted to have slightly increased temperature, in a linear pattern after the dorsal spinal processes represented by the color white and red and surrounded by a cooler color pattern in the regions more laterally as represented by the darker colors (Fig 3). Dogs with TLIVDD had a similar pattern, but with a more focal elevation in temperature represented by a "white spot" in the region above the herniated intervertebral disk (Fig 4). A study describing the thoracolumbar MII in horses reports a similar linear warmer temperature pattern found midline and a cooler pattern laterally from the spinal column.[43] Speculation that naturally occurring increased density of superficial subcuticular blood vessels was the cause of the midline linear pattern of increased temperature was cited; however, no documentation of such a vascular pattern could be found in the horse or the dog. Because the natural hairline parts on midline in both species, more skin is exposed on midline than in regions lateral to midline where hair shafts begin to overlap. Hair is a natural insulator and its effect on MII, namely insulating the body from heat loss, thus lowering the temperature reading without altering the thermographic pattern, has been reported in the dog.[37,41] Because temperature measurements in regions of sparse hair coat are derived directly from the skin rather than through an intact hair coat, they are expected to be slightly higher along midline as is found in both the axillary and inguinal regions of dogs.[37]

When the dorsal images were divided into ROI for purposes of localization of the intervertebral disk protrusion using computer recognition pattern analysis, 97% of the vertebral segments were correctly classified as affected, versus non-affected by TLIVDD, when compared with MRI and surgical findings. The disk space affected was represented by a

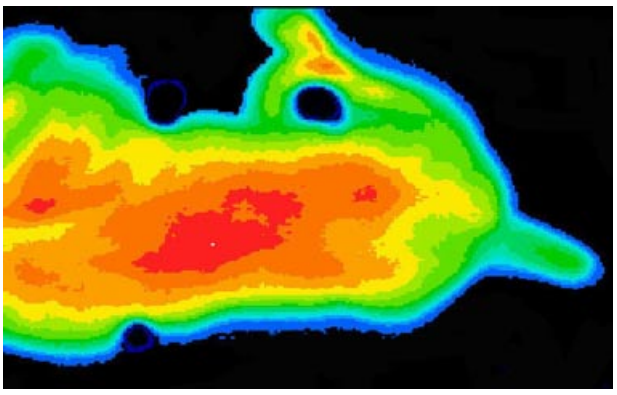

Figure 3 Medical infrared image of the dorsal view of a 1-year-old male neutered Chihuahua with no evidence of neurologic disease on physical or MRI examination.

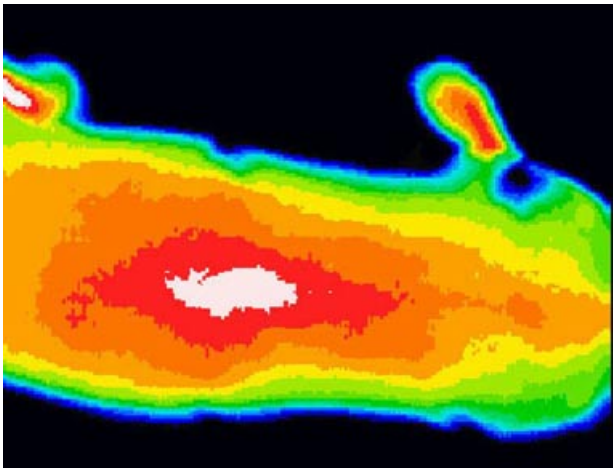

Figure 4 Medical infrared image of the dorsal view of a 6-year-old female spayed Dachshund with grade 2 neurologic deficits secondary to a herniated intervertebral disc at T12–13 on the right. Note the focal elevation in temperature in the region of the affected disc space (arrow).

focal area of hyperthermia as was reported in horses with neurologic injury.[38,48] These findings are consistent with the results of a study in people with cervical IVDD where MII not only correctly identified disk herniation but the location as well.[26] It is important to recognize that other pathologic changes can affect the thermographic image, and MII cannot determine the cause of the abnormal pattern. Studies are ongoing to assess the utility of MII in differentiating chronic versus acute TLIVDD and other pathologic conditions (neoplasia, inflammation). Dogs with TLIVDD may have multiple sites of intervertebral disk degeneration, bulging of the intervertebral disk, and disk protrusion that may not be associated with clinical signs.[7] MII may prove a useful adjunct to MRI in assisting the clinician in differentiating clinical TLIVDD from subclinical TLIVDD in dogs with more than 1 lesion found on MRI. Additionally, MII may be useful for evaluating lesions affected the cervical spine or peripheral neurologic disease. It may also provide an objective method to measure responses to traditional and alternative treatments for compressive lesions of the spinal cord including TLIVDD. Additional studies would be warranted to investigate these potential applications of MII. Finally, myelography, CT, and MRI require general anesthesia and pose inherent risk especially in patients with cardiac, renal, or hepatic insufficiency.[51–54] Because MII does not require sedation or anesthesia, patients with associated anesthetic or contrast administration risk factors can be imaged safely.

Recheck Evaluation

No significant difference was found when comparing ROI mean temperature between the pre- and postoperative measurements in dogs with TLIVDD. When comparing CRPA, significant overlap in pattern analysis was noted comparing the recheck group to the clinical and control groups. Some overlap in the images is to be expected, and the fact that

the recheck group more closely resembled the clinical group may indicate that the experimental time frame was not long enough to allow complete resolution of the abnormal thermographic pattern. Whereas the mean neurologic grade of the recheck group was lower than the clinical group, it was not normal. It is possible that the persistent alteration in thermographic pattern may correspond to the residual neurologic status after surgery. Alternatively, it may be possible that the thermal imaging pattern of a dog that has had decompressive surgery may never return to the normal pattern. We arbitrarily selected 10 weeks postoperatively to re-assess dogs with MII. Further studies would be needed to determine when the thermographic patterns of the clinical dogs return to normal or if abnormal patterns persist. Studies are in progress to correlate MII findings with clinical outcome in an effort to determine the utility of MII as a prognostic tool. In people, thermographic regions of asymmetry and temperature differences have been documented on the distal extremities based on intervertebral disk lateralization and subsequent nerve root compression.[23,26,55–57] Data analysis is ongoing to determine the utility of MII in the identifying the side of IVD compression compared with MRI and surgical findings.

Limitations of our study were related to the number and breed distribution of dogs in the experimental groups and the limited follow-up. There was poor owner compliance with the 10-week MII re-imaging resulting in only 21 dogs being assessed. It is not known if the findings would be similar in larger dogs or if findings would be different in the cervical region. Additionally, multiple disk spaces were decompressed to ensure complete removal of extruded disk material in some dogs at the discretion of the surgeon. Multiple adjacent surgical sites, partial decompression of the chronic portion of the IVDD may have altered the interpretation of the follow-up MII. Finally, longer follow-up times may have revealed additional resolution of the thermographic pattern abnormalities. It is currently unknown if dogs that have spinal surgery will ever regain a completely normal imaging pattern.

Whereas MII was successful in identifying dogs affected with TLIVDD and localizing the site of intervertebral disk protrusion, it is not a specific test with regard to the type of pathology present. It serves as a screening test for the presence or absence of pathology in a minimally invasive manner. Further studies are needed to determine the role of MII in assessing patient recovery and prognosis.

DISCLOSURE

The authors report no financial or other conflicts related to this report.

REFERENCES

1. Jerram RM, Dewey CW: Acute thoracolumbar disk extrusion in dogs—part 1. *Compend Contin Educ Pract Vet* 1999;21:922–930
2. Jerram RM, Dewey CW: Acute thoracolumbar disk extrusion in dogs—part II. *Compend Contin Educ Pract* 1999;21:1037–1047
3. Griffin JF, Levine JM, Kerwin SC: Canine thoracolumbar disk disease: pathophysiology, neurologic examination, and emergency medical therapy. *Compendium Online* 2009;31:E2
4. Dewey CW: Myelopathies: disorders of the spinal cord, in: Dewey CW (ed): *A practical guide to canine and feline neurology* (ed 2). Ames, IA, Iowa State Press, 2008, pp 323–388
5. Hansen HJ: A pathologic-anatomic study on disk degeneration in the dog, with special reference to the so-called enchondrosis intervertebralis. *Acta Orthop Scand Suppl* 1952;11:1–117
6. Toombs JP, Waters DJ: Intervertebral disc disease, in Slatter D (ed): *Textbook of small animal surgery* (ed 3). Philadelphia, PA, Saunders, 2003, pp 1193–1209
7. Besalti O, Pekcan Z, Sirin YS, et al: Magnetic resonance imaging findings in dogs with thoracolumbar intervertebral disk disease: 69 cases (1997–2005). *J Am Vet Med Assoc* 2006;228:902–908
8. Priester WA: Canine intervertebral disk disease-occurrence by age, breed, and sex among 8117 cases. *Theriogenology* 1976;6:293–303
9. de Lahunta A, Glass E (eds): Small animal spinal cord disease, in: *Veterinary neuroanatomy and clinical neurology* (ed 3). St. Louis, MO, Saunders Elsevier, 2009, pp 243–284
10. Ito D, Matsunaga S, Jeffery ND, et al: Prognostic value of magnetic resonance imaging in dogs with paraplegia caused by thoracolumbar intervertebral disk extrusion: 77 cases (2000–2003). *J Am Vet Med Assoc* 2005;227:1454–1460
11. Bagley RS, Tucker R, Harrington ML: Lateral and foraminal disk extrusion in dogs. *Comp Cont Vet Med Ed* 1996;18:795–804
12. Naude SH, Lambrechts NE, Wagner WM, et al: Association of preoperative magnetic resonance imaging findings with surgical features in Dachshunds with thoracolumbar intervertebral disk extrusion. *J Am Vet Med Assoc* 2008;332:702–708
13. Tartarelli CL, Baroni M, Borgh M: Thoracolumbar disk extrusion associated with epidural haemorrhage: a retrospective study of 23 dogs. *J Small Anim Pract* 2005;46:485–490
14. Eddy AL, Van Hoogmoed LM, Snyder JR: The role of thermography in the management of equine lameness. *Vet J* 2001;162:172–181
15. Love TJ: Thermography as an indicator of blood perfusion. *Ann NY Acad Sci* 1980;335:429–437
16. Turner TA: Thermography as an aid to the clinical lameness evaluation. *Vet Clin N Am Equine Pract* 1991;7:311–338
17. Leandro P: *Meditherm manual of clinical thermology.* Beaufort, NC, Meditherm, 2004
18. Head JF, Elliott R: Infrared imaging: making progress in fulfilling it's medical promise. *IEEE Eng Med Biol Mag* 2002;21:80–85
19. Gratt BM, Sickles EA, Wexler CE: Thermographic characterization of osteoarthrosis of the temporomandibular joint. *J Orofacial Pain* 1993;7:345–353
20. Mangine RE, Siqueland KA, Noyes FR: The use of thermography 398 for the diagnosis and management of patellar tendinitis. *J Orthop Sports Phys Ther* 1987;9:132–140
21. Ring EF, Dieppe PA, Bacon PA: The thermographic assessment of inflammation and anti-inflammatory drugs in osteoarthritis. *Brit J Clin Prac* 1981;35:263–264
22. Devereaux MD, Parr GR, Lachmann SM, et al: Thermographic diagnosis in athletes with patellofemoral arthralgia. *J Bone Joint Surg Br* 1986;68:42–44

23. Pochaczevsky R, Wexler CE, Meyers PH, et al: Liquid crystal thermography of the spine and extremities. *J Neurosurg* 1982;56:386–395
24. Maigne JY, Treuil C, Chatellier G: Altered lower limb vascular perfusion in patients with sciatica secondary to disk herniation. *Spine* 1996;21:1657–1660
25. Doman I, Illes T: Thermal analysis of the human intervertebral disk. *J Biomech Biophys Methods* 2004;61:207–214
26. Zhang HY, Kim YS, Cho YE: Thermatomal changes in cervical disk herniations. *Yonsei Med J* 1999;40:401–412
27. Plaugher G: Skin temperature assessment for neuromusculoskeletal abnormalities of the spinal column. *J Manipulative Physiol Ther* 1992;15:365–381
28. Gautherie M, Haehnel P, Walter J, et al: Thermovascular changes associated with in situ and minimal breast cancers. *J Reprod Med* 1987;32:833–842
29. Verheye S, DeMeyer GR, Krams R, et al: Intravascular thermography: immediate functional and morphological vascular findings. *Eur Heart J* 2004;25:158–165
30. Clark JA: The potential of infra-red thermography in veterinary diagnosis. *Vet Rec* 1977;100:402–404
31. Schaefer AL, Cook NJ, Church JS, et al: The use of infrared thermography as an early indicator of bovine respiratory disease complex in calves. *Res Vet Sci* 2007;83:376–384
32. Rainwater-Lovett K, Pacheco JM, Packer C, et al: Detection of foot-and-mouth disease virus infected cattle using infrared thermography. *Vet J* 2009;180:317–324
33. Colak A, Polat B, Okumus Z, et al: Short communication: early detection of mastitis using infrared thermography in dairy cows. *J Dairy Sci* 2008;91:4244–4248
34. Heath AM, Carson RL, Purohit RC, et al: Effects of testicular biopsy in clinically normal bulls. *J Am Vet Med Assoc* 2002;220:507–512
35. Heath AM, Pugh DG, Sartin EA, et al: Evaluation of the safety and efficacy of testicular biopsies in llamas. *Theriogenology* 2002;58:1125–1130
36. Purohit RC, Carson RL, Riddell MG, et al: Peripheral neurogenic thermogenic thermoregulation of the bovine scrotum. *Thermol Int* 2007;17:138–142
37. Loughin CA, Marino DJ: Evaluation of thermographic imaging of the limbs of healthy dogs. *Am J Vet Res* 2007;68:1064–1069
38. Turner TA: Diagnostic thermography. *Vet Clin North Am Equine Pract* 2001;17:95–113
39. Marino DJ, Loughin CA: Diagnostic imaging of the canine stifle: a review. *Vet Surg* 2010;39:284–295
40. Purohit RC: Use of thermography in veterinary medicine, in: Lee MHM, Cohen JM (eds): *Rehabilitation medicine and thermography.* Wilsonville, OR, Impress Publications, 2008, pp 129–141
41. Infernuso T, Loughin CA, Marino DJ, et al: Thermal imaging of normal and cranial cruciate ligament-deficient stifles in dogs. *Vet Surg* 2010;39:410–417
42. Um SW, Kim MS, Lim JH, et al: Thermographic evaluation for the efficacy of acupuncture on induced chronic arthritis in the dog. *J Vet Med Sci* 2005;67:1283–1284
43. Tunley BV, Henson FMD: Reliability and repeatability of thermographic examination and the normal thermographic image of the thoracolumbar region in the horse. *Equine Vet J* 2004;36:306–312
44. Fonseca BPA, Alves ALG, Nicoletti JLM, et al: Thermography and ultrasonography in back pain diagnosis of equine athletes. *J Equine Vet Sci* 2006;26:507–516
45. Purohit RC, McCoy MD: Thermography in the diagnosis of inflammatory processes in the horse. *Am J Vet Res* 1980;41:1167–1174
46. Schweinitz DG: Thermographic evidence for the effectiveness of acupuncture in equine neuromuscular disease. *Acupunct Med* 1998;16:15–17
47. Steiss J: Coccygeal muscle injury in English Pointers (limber tail). *J Vet Int Med* 1999;13:540–548
48. Purohit RC, McCoy MD, Bergfeld WA: Thermographic diagnosis of Horner's syndrome in the horse. *Am J Vet Res* 1980;41:1180–1182
49. Kim WT, Kim MS, Kim SY, et al: Use of digital infrared thermography on experimental spinal cord compression in dogs. *J Vet Clin* 2005;22:302–308
50. Wheeler SJ, Sharp NJ: Patient examination, in: Wheeler SJ, Sharp NJH (eds): *Small animal spinal diagnosis: diagnosis and surgery* (ed 2). Philadelphia, PA, Mosby Yearbook, London, 2005, pp. 19–33
51. Barone G, Ziemer LS, Shofer FS, et al: Risk factors associated with development of seizures after use of iohexol for myelography in dogs: 182 cases (1998). *J Am Vet Med Assoc* 2002;220:1499–1503
52. Lexmaulova L, Zatloukal J, Proks P, et al: Incidence of seizures associated with iopamidol or iomeprol myelography in dogs with intervertebral disk disease: 161 cases (2000–2002). *J Vet Emerg Crit Care* 2009;19:611–616
53. Kishimoto M, Yamada K, Euno H, et al: Spinal cord effects from lumbar myelographic injection technique in the dog. *J Vet Med Sci* 2004;66:67–69
54. Packer RA, Bergman RL, Coates JR, et al: Intracranial subarachnoid hemorrhage following lumbar myelography in two dogs. *Vet Radiol Ultrasound* 2007;48:323–327
55. So YT, Aminoff MJ, Olney KO: The role of thermography in the evaluation of lumbosacral radiculopathy. *Neurology* 1989;39:1154–1158
56. So YT, Olney RK, Aminoff MJ: Evaluation of thermography in the diagnosis of selected entrapment neuropathies. *Neurology* 1989;39:1–5
57. Kim YC, Bahk JH, Lee SC, et al: Infrared thermographic imaging in the assessment of successful block on lumbar sympathetic ganglion. *Yonsei Med J* 2003;44:119–124

SUPPORTING INFORMATION

Additional supporting information may be found in the online version of this article at the publisher's website.

Table S1. Summary of the Data From the Regions of Interest in the Control and in Dogs With TLIVDD